Boundary conditions in multiband $k\cdot p$ models: A tight-binding test

Silvano De Franceschi, Jean-Marc Jancu, and Fabio Beltram
Scuola Normale Superiore and INFM, I-56126 Pisa, Italy
(Received 8 October 1998)

A quantitative comparison between different $\boldsymbol{k}\cdot\boldsymbol{p}$ calculations of valence-band states in quantum-confinement semiconductor heterostructures is presented. The importance of using appropriate boundary conditions to match the envelope functions across abrupt heterointerfaces is addressed quantitatively using an improved tight-binding model to discriminate between existing models. The relevance of the present results to the design of optoelectronic devices is discussed. [S0163-1829(99)11015-4]

The envelope-function approximation (EFA) is widely employed in the design of semiconductor heterostructures because of its straightforward applicability and its limited computational effort.[1,2] The fundamental assumptions on which it is founded and the exact knowledge of the limits of its applicability have always been a matter of considerable debate.[3–9] One of the main problems is the choice of appropriate boundary conditions to match the envelope functions across semiconductor heterointerfaces.

In most cases the EFA is implemented as an effective-mass equation for the whole heterostructure, which also holds across abrupt interfaces. Away from them, equations reduce to the usual bulk form. This description was originally based on heuristic arguments,[2,10–13] but was formalized into an exact envelope-function theory by Burt about a decade ago.[3,4] Envelope-function components are continuous everywhere and boundary conditions for their derivatives can be obtained by integration of the effective-mass equation across the heterointerface.[14] The interface connection rules thus depend on the explicit form of the Hamiltonian operator. Different forms were considered,[11,16,17] the most widely used being based on the symmetrization of the bulk Hamiltonian as discussed in the following. Correct guidelines for the derivation of the $\boldsymbol{k}\cdot\boldsymbol{p}$ heterostructure Hamiltonian were given by Burt in.[3,4] Following these lines Foreman has derived a three-band effective-mass Hamiltonian for the valence band which has been shown to provide more plausible results compared to the more widely used symmetrized model.[13,15] However, a clear quantitative test of the accuracy of Foreman's model is still lacking.

This issue is addressed in the present paper with the aid of a recently developed tight-binding (TB) model. We focus on the case of III-V heterostructures with barrier and well materials with different effective-mass parameters. We show that Foreman's Hamiltonian always leads to energy-dispersion relations in good agreement with TB calculations, while the ''symmetrized'' Hamiltonian does not. We also discuss the implications of the present results to the design of heterostructures relevant to device applications.

For a semiconductor heterostructure under external fields depending on z only (we take z as the growth axis) the multiband effective-mass equation takes the general form:

$$\sum_{s'} \hat{H}_{ss'}(z) f_{s'}(z) = E f_s(z), \tag{1}$$

where $f_s(z)$ are the z-dependent components of the envelope function and $\hat{H}_{ss'}(z)$ is the effective-mass operator. As far as valence-band states are considered $\hat{H}_{ss'}(z)$ can be explicitly written as[4]

$$\hat{H}_{ss'}(z) = \sum_{\alpha,\beta\neq 3} \gamma_{ss'}^{\alpha\beta}(z) k_\alpha k_\beta + \hat{k}_3 \sum_{\beta\neq 3} \gamma_{ss'}^{3\beta}(z) k_\beta + \sum_{\alpha\neq 3} k_\alpha \gamma_{ss'}^{\alpha 3}(z) \hat{k}_3 + \hat{k}_3 \gamma_{ss'}^{33}(z) \hat{k}_3 + \zeta_{ss'}(z). \tag{2}$$

Wave-vector components have the following notation: $k_1 = k_x$, $k_2 = k_y$, $\hat{k}_3 = -i\nabla_z$. $\gamma_{ss'}^{\alpha\beta}(z)$ are coefficients of the kinetic tensor and reflect the band-structure properties of the bulk material at z. Matrix elements $\zeta_{ss'}(z)$ represent the potential part of the Hamiltonian describing the band-edge profile and possible strain effects. $f_s(z)$ are continuous whereas the matching conditions for their first derivatives are obtained by integrating the effective-mass equation across every heterointerface. This procedure leads to the following continuity relation for an interface at $z=0$:

$$\sum_{s'} \left(\sum_{\beta\neq 3} \gamma_{ss'}^{3\beta}(-\epsilon) k_\beta + \gamma_{ss'}^{33}(-\epsilon) \hat{k}_3 \right) f_{s'}(-\epsilon) = \sum_{s'} \left(\sum_{\beta\neq 3} \gamma_{ss'}^{3\beta}(\epsilon) k_\beta + \gamma_{ss'}^{33}(\epsilon) \hat{k}_3 \right) f_{s'}(\epsilon). \tag{3}$$

We note that this boundary condition fulfills the requirement of current conservation, as discussed in Ref. 4.

As mentioned above, the most widespread approach in deriving the heterostructure effective-mass operator is based on the simple substitution of $k_3 (= k_z)$ with $\hat{k}_3$ in the bulk Hamiltonian. That is done after a preliminary symmetrization with respect to k_3, i.e., terms like $\eta(z) k_3$ are replaced by $(1/2)[\eta(z)\hat{k}_3 + \hat{k}_3 \eta(z)]$, while $\eta(z) k_3^2$ is rewritten as $\hat{k}_3 \eta(z) \hat{k}_3$.[2,11,12] This procedure (which is not the only option ensuring the hermiticity of the effective-mass operator[16,17]) is equivalent to assume $\gamma_{ss'}^{\alpha 3} = \gamma_{ss'}^{3\alpha}$ in Eq. (2). The arbitraryness of this assumption has important implications on the boundary conditions and can cause significant inaccuracies in the calculation of quantized electronic states. As a direct conse-

quence spectral functions (such as density of states, optical gain, etc.) in low-dimensional structures can be poorly described within the EFA if this ''symmetrized'' model is adopted.

We consider this problem quantitatively for the case of valence-band states in III-V heterostructures. We refer to three-band $\boldsymbol{k}\cdot\boldsymbol{p}$ models including heavy-hole, light-hole, and spin-orbit split-off bands. For simplicity we restrict our discussion to single-quantum-well heterostructures. We want to compare the results obtained using the most common approach described above with those given by a ''nonsymmetrized'' model in which the effective-mass coefficients $\gamma_{ss'}^{\alpha\beta}$ in Eq. (2) have been derived from perturbation theory with no arbitrary assumptions (see Ref. 13). In bulk materials, the two models are indistinguishable with the kinetic tensor in Eq. (2), reducing to the 6×6 Luttinger-Kohn form.[18] In quantum heterostructures, the two models give identical results at the Brillouin-zone center but different in-plane dispersion relations. This stems from a difference in the resulting boundary conditions on the first derivative of the envelope-function components. In particular, the ''symmetrized'' model overestimates the coupling between subbands of different character, which is represented by the off-diagonal terms in Eq. (3).[13] It can be noted that the larger the difference between the effective-mass parameters of the barrier and the well, the stronger is this coupling, and therefore the disagreement between the results of the two models.

In order to test their accuracy we performed band-structure calculations within the TB approximation using a 40-band empirical $sp^3d^5s^*$ nearest-neighbor model that includes spin-orbit coupling.[19] This TB model adequately reproduces measured effective masses, interband transition energies, and deformation potentials of III-V semiconductors and provides a precise description of electronic states in short-period superlattices and quantum wells.[20,21]

In order to ensure a meaningful comparison, bulk-material parameters used in both $\boldsymbol{k}\cdot\boldsymbol{p}$ models (i.e., Luttinger parameters, split-off energy, deformation potentials) were set by fitting the TB bulk-band structures.

Figure 1 shows our calculations for the valence-band structure of a 4.8-nm thick GaAs/AlAs single quantum well (QW) grown on a GaAs(001) substrate. The in-plane dispersion relation along both [100] and [110] directions is shown for the uppermost subbands. Solid and dashed lines refer to the ''nonsymmetrized'' and ''symmetrized'' model, respectively, while the results of TB calculations are represented by filled circles (note that spin degeneracy is lifted in TB subbands by the lack of inversion symmetry of the host unit cells, which is instead neglected in the present $\boldsymbol{k}\cdot\boldsymbol{p}$ models[22]). As expected, the two sets of $\boldsymbol{k}\cdot\boldsymbol{p}$ subbands coincide at the Brillouin-zone center. They do not show pronounced discrepancies at nonzero in-plane k vectors. This follows from the rather small difference between the effective-mass parameters of GaAs and AlAs. The ''nonsymmetrized'' model, however, is seen to give the best agreement with TB results. In particular, a very good consistency over the whole range of k vectors shown is found for the ground subband. The latter is often the most important one in determining the measured heterostructure properties. Indeed the ''symmetrized'' model leads to fairly small deviations from the TB results: this is a direct evidence of why such a model was used so widely and successfully in this material system.

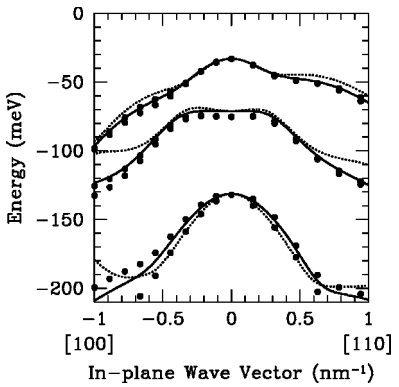

FIG. 1. Valence band structure of a 17 molecular-layer-thick GaAs/AlAs quantum well grown on GaAs(001). Calculated in-plane dispersion relations along [100] and [110] are shown in the left and right part of the figure, respectively. Energy is refered to the bulk valence-band edge of the quantum-well material. Solid (dashed) lines are obtained with the ''nonsymmetrized'' (''symmetrized'') three-band $\boldsymbol{k}\cdot\boldsymbol{p}$ model described in the text. Tight-binding (TB) results are represented by filled circles. Effective-mass parameters entering $\boldsymbol{k}\cdot\boldsymbol{p}$ models were chosen in order to ensure the best agreement with TB results for the bulk valence-band structure of the costituent materials. In particular, we set $\gamma_1=7.05$, $\gamma_2=2.0$, and $\gamma_3=3.0$ for GaAs and $\gamma_1=3.88$, $\gamma_2=0.69$, and $\gamma_3=1.46$ for AlAs. A valence-band offset of 0.5 eV was assumed in these calculations.

In the following figures we show that this scenario drastically changes when barrier and well materials with more dissimilar effective-mass parameters are considered. Figure 2 shows the in-plane dispersion relation for the valence subbands of a strained 5.1-nm thick GaSb/AlSb QW grown on AlSb(001). The biaxial tensile strain in the QW material arises from the lattice mismatch (0.65%) between GaSb and AlSb, and splits the degeneracy between the light-hole and heavy-hole bulk-band edges pushing the latter below the former. As a result of the combined effect of strain and quantum confinement, the first two subbands are nearly degenerate at the Brillouin-zone center and strongly coupled at relatively small nonzero k vectors due to the off-diagonal terms in Eq. (3). Under these conditions large discrepancies between the two $\boldsymbol{k}\cdot\boldsymbol{p}$ models emerge, especially with regard to the ground subband. As shown if Fig. 2, the ''symmetrized'' model yields a more pronounced electronlike character at the Brillouin-zone center and a valence-band maximum significantly higher ($\sim$20 meV) in energy. Instead, the results of the ''nonsymmetrized'' model are in good agreement with TB calculations over the whole k-vector range shown.

A similar situation is presented in Fig. 3 for the case of a tensily strained 5.7-nm thick $In_{0.43}Ga_{0.57}As/InP$ QW grown on InP(001). There is much technological interest on $In_{0.43}Ga_{0.57}As/InP$ heterostructures owing to their many optoelectronics applications. By varying In content above or below the lattice-matching value (53%) either compressive or tensile deformation, respectively, can be induced in pseudomorphic $In_{0.43}Ga_{0,57}As$ QW's. This additional degree

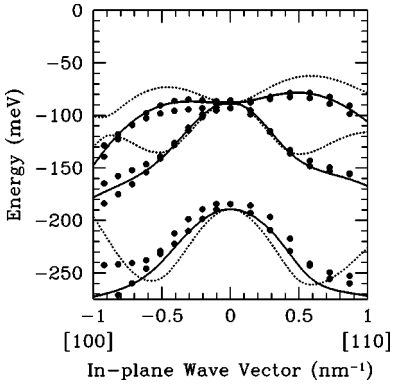

FIG. 2. Valence band structure of a 17 molecular-layer-thick GaSb/AlSb tensily strained quantum well lattice matched on AlSb(001): Calculated in-plane dispersion relations along [100] and [110] are shown in the left and right part of the figure, respectively. Energy is refered to the bulk valence-band edge of the quantum-well-material. Solid (dashed) lines are obtained with the ''nonsymmetrized'' (''symmetrized'') three-band $\boldsymbol{k\cdot p}$ model described in the text. Tight-binding (TB) results are represented by filled circles. Effective-mass parameters entering $\boldsymbol{k\cdot p}$ models were chosen in order to ensure the best agreement with TB results for the bulk valence-band structure of the costituent materials. In particular, we set $\gamma_1=12.0$, $\gamma_2=4.0$, and $\gamma_3=5.3$ for GaSb and $\gamma_1=5.4$, $\gamma_2=1.14$, and $\gamma_3=2.22$ for AlSb. The valence-band offset value between unstrained GaSb and AlSb was taken at 0.4 eV.

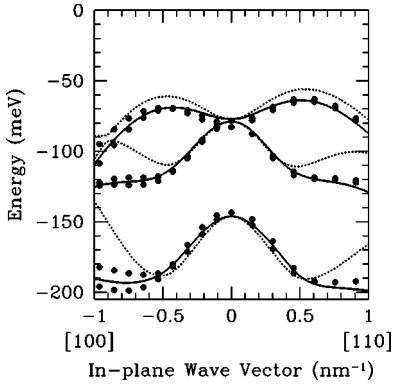

FIG. 3. Valence-band structure of a 20 molecular-layer-thick $In_{0.43}Ga_{0.57}As/InP$ tensily strained quantum well lattice-matched on InP(001). Calculated in-plane dispersion relations along [100] and [110] are shown in the left and right part of the figure, respectively. Energy is refered to the bulk valence-band edge of the quantum-well material. Solid (dashed) lines are obtained with the ''nonsymmetrized'' (''symmetrized'') three-band $\boldsymbol{k\cdot p}$ model described in the text. Tight-binding (TB) results are represented by filled circles. Effective-mass parameters entering $\boldsymbol{k\cdot p}$ models were chosen in order to ensure the best agreement with TB results for the bulk valence-band structure of the costituent materials. In particular, we set $\gamma_1=10.2$, $\gamma_2=3.60$, and $\gamma_3=4.55$ for $In_{0.43}Ga_{0.57}As$ and $\gamma_1=6.25$, $\gamma_2=1.87$, and $\gamma_3=2.65$ for InP. The value of the valence-band offset between unstrained $In_{0.43}Ga_{0.57}As$ and InP was taken at 0.32 eV.

of freedom has proved very useful to improve the performance of a variety of devices.[23–27] Our results shown in Fig. 3 point at the importance of using an appropriate $\boldsymbol{k\cdot p}$ model to accurately design quantum-heterostructure devices in the $In_{0.43}Ga_{0.57}AsP$ material system. TB calculations demostrate that the ''nonsymmetrized'' model is the valid option.

We should like to compare our results with those obtained by Yamanaka *et al.*[28] for very similar material systems. These authors pointed at some anomalies in the in-plane dispersion relation of valence states calculated with a 4×4 symmetrized model. Such anomalies were linked to the continuity requirement on the envelope functions. Alternative connection rules were therefore proposed to handle interfaces between materials of substantially different effective-mass parameters. Our results, on the contrary, show on a quantitative base that the usual approach to boundary conditions is appropriate also in the case of different material parameters provided the correct form of the Hamiltonian operator is employed.

A recent paper by Meney *et al.*[15] showed that the inclusion of the lowest conduction band in symmetrized Hamiltonians can lead to anomalous deviations in the calculated dispersion relation. The ''nonsymmetrized'' approach does not exhibit this unphysical behavior and, as shown in Figs. 2 and 3, accurate results can be obtained without explicitly including the conduction band.

In conclusion, we have analyzed the role of boundary conditions in the calculation of the valence-band structure of single QW's within the EFA. Two three-band $\boldsymbol{k\cdot p}$ models were considered: the most commonly used ''symmetrized'' model and a ''nonsymmetrized'' one resulting from a rigorous derivation of the Hamiltonian operator. The direct comparison with a recently developed TB approach allowed us to discriminate in favor of the latter, which was shown to yield reliable results also when barrier and well materials have very dissimilar effective-mass parameters. Finally, we have emphasized the relevance of the model discrepancies in the design of devices such as those based on $In_{0.43}Ga_{0,57}As/InP$ and GaSb/AlSb quantum heterostructures.

We acknowledge L. C. Andreani, V. Pellegrini, and G. La Rocca, for valuable discussions. This paper was supported in part by INTAS under Project No. 94-1172.

[1] G. Bastard, *Wave Mechanics Applied to Semiconductors Heterostructures* (Les Editions de Physique, Les Ulis, 1988), p. 63; D. Smith and C. Mailhiot, Rev. Mod. Phys. **62**, 173 (1990).
[2] M. Altarelli, in *Heterojunctions and Semiconductor Superlattices*, edited by G. Allan, G. Bastard, N. Boccora, and M. Voos (Springer, Berlin, 1986).
[3] M. G. Burt, Semicond. Sci. Technol. **3**, 739 (1988).
[4] M. G. Burt, J. Phys.: Condens. Matter **4**, 6651 (1992).
[5] T. Ando, S. Wakahara, and H. Akera, Phys. Rev. B **40**, 11 609 (1989).
[6] R. Winkler and U. Rössler, Phys. Rev. B **48**, 8918 (1993).
[7] G. T. Einevoll and L. J. Sham, Phys. Rev. B **49**, 10 533 (1994).
[8] D. M. Wood and A. Zunger, Phys. Rev. B **53**, 7949 (1996).
[9] B. A. Foreman, Phys. Rev. Lett. **80**, 3823 (1998).

[10] G. Bastard, Phys. Rev. B **24**, 5693 (1981).
[11] W. Pötz, W. Porod, and D. K. Ferry, Phys. Rev. B **32**, 3868 (1985).
[12] R. Eppenga, M. F. H. Schuurmans, and S. Colak, Phys. Rev. B **36**, 1554 (1987).
[13] B. A. Foreman, Phys. Rev. B **48**, 4964 (1993).
[14] Note that by definition exact envelope functions and their derivative are continuous. Discontinuities in the derivatives, however, can arise at the heterojunction when the effective-mass approximation is used (see Ref. 4).
[15] A. T. Meney, Besir Gonul, and E. P. O'Reilly, Phys. Rev. B **50**, 10 893 (1994).
[16] R. A. Morrow and K. R. Brownstein, Phys. Rev. B **30**, 678 (1984).
[17] G. T. Einevoll, P. C. Hemmer, and J. Thomsen, Phys. Rev. B **42**, 3485 (1990).
[18] J. M. Luttinger and W. Kohn, Phys. Rev. **97**, 869 (1955).
[19] J. M. Jancu, R. Scholz, F. Beltram, and F. Bassani, Phys. Rev. B **57**, 6493 (1998).
[20] R. Scholz, J.-M. Jancu, and F. Bassani, in *Tight-Binding Approach to Computational Materials Science*, edited by P. E. A. Turchi, A. Gonis, and L. Colombo, MRS Symposia Proceedings No. 491 (Materials Research Society, Pittsburgh, 1998), pp. 383–388.
[21] J.-M. Jancu, V. Pellegrini, R. Colombelli, F. Beltram, B. H. Müller, L. Sorba, and A. Franciosi, Appl. Phys. Lett. **73**, 2621 (1998).
[22] D. L. Smith and C. Maillot, Rev. Mod. Phys. **62**, 173 (1990).
[23] D. Ahn, S. J. Yoon, S. L. Chuang, and C.-S. Chang, J. Appl. Phys. **78**, 2489 (1995).
[24] M. P. C. M. Krijn *et al.*, Appl. Phys. Lett. **61**, 1772 (1992).
[25] L. F. Tiemeijer, P. J. A. Thijs, P. J. de Waard, J. J. M. Binsma, and T. v. Dongen, Appl. Phys. Lett. **58**, 2738 (1991).
[26] G. Lenz, E. P. Ippen, J. M. Wiesenfeld, M. A. Newkirk, and U. Koren, Appl. Phys. Lett. **68**, 2933 (1996).
[27] T. Schwander *et al.*, Appl. Phys. Lett. **70**, 2855 (1997).
[28] T. Yamanaka, H. Kamada, Y. Yoshikuni, W. W. Lui, S. Seki, and K. Yokoyama, J. Appl. Phys. **76**, 2347 (1994).